# MEASUREMENTS OF UNDERWATER EXPLOSION PERFORMANCES BY PRESSURE GAUGE USING FLUOROPOLYMER

Kenji MURATA, Katsuhiko TAKAHASHI, Yukio KATO*
NOF Corporation
61-1 Kitakomatsudani, Taketoyo-cho, Chita-gun, Aichi 470-2398, JAPAN

Pressure gauge using fluoropolymer as sensing element was developed to measure underwater shock wave profile at the location very close to the explosive-water boundary. Shock wave profile was successfully measured in high pressure range where peak shock wave pressure exceeded 400MPa for emulsion explosives and aluminized emulsion explosives. First bubble pulse profile was also precisely measured by pressure gauge using fluoropolymer. The experimental results shows that the late energy release by aluminum reaction in detonation products enhanced both shock wave and first bubble pulse. It is demonstrated that the impulse of first bubble pulse is about 2.5 times greater than shock wave impulse, although peak pressure of first bubble pulse is only 10~15% of peak shock wave pressure.

## INTRODUCTION

During last decades, the underwater explosion test has contributed appreciably to understand the detonation effects of explosives in terms of their measured underwater shock and bubble effects[1,2]. The underwater explosion test has some advantages over other experimental techniques such as pressure measurements, particle velocity measurements and cylinder test, because large mass of surrounding water provides sufficient confinement to maintain detonation products at high pressure, and allows to observe the state of detonation products at different pressure and time range. Particularly, in the case of aluminized explosives, sufficient confinement realized in the underwater explosion test enables relatively slow aluminum reaction to complete in detonation products.

In the engineering applications such as shock forming of metal plates and shock consolidation of metallic and ceramic powders etc, the measurements of underwater shock wave in high pressure range are required to control shock wave loading on target samples. To understand destructive effects of underwater explosion phenomena, it is also important to measure precisely bubble pulse as well as shock wave.

Underwater shock wave and bubble pulse have been widely measured by pressure gauge using tourmaline crystal. However, maximum measurable pressure is limited to pressure lower than 100 MPa, because tourmaline crystal is destroyed by high pressure generated due to the impedance mismatch with water. Pressure gauge using fluoropolymer has potentially the possibility to measure high underwater shock pressure (> 100 MPa), since shock impedance of fluoropolymer is very close to that of water. In our previous studies[3,4], we developed a pressure gauge using

---

*Guest Professor of Shock Wave and Condensed Matter Research Center, Kumamoto University

fluoroplymer as sensing element, which can measure underwater shock wave pressure higher than 100 MPa. In the measurements of bubble phenomena by tourmaline gauge, a shift in bubble pulse base line to negative pressure after the passage of shock wave is observed. This deviation of bubble pulse base line to negative pressure makes the precise quantitative measurements of bubble pulse difficult. It is demonstrated that pressure gauge using fluoropolymer can maintain base line of bubble pulse after the passage of shock wave, and permits precise measurements of bubble pulse[5].

In this study, underwater shock wave and bubble pulse were measured by pressure gauge using fluoropolymer for the emulsion explosives (EMX) and aluminized emulsion explosives (AL-EMX). It was demonstrated that pressure gauge using fluoropolymer can measure underwater shock wave profile in the pressure range higher than 400 MPa. Peak pressure and impulse of first bubble pulse were precisely measured and compared with those of shock wave. It was shown that aluminum reaction enhanced shock wave energy, shock wave impulse, first bubble impulse and bubble energy.

## EXPERIMENTAL

Properties of sample explosives EMX and AL-EMX are shown in Table 1.

Composition of base emulsion matrix was consisted of 74.6wt% of ammonium nitrate, 10.6wt% of hydrazine nitrate, 10.6wt% of water, 4.2wt% of wax and emulsifier. Formed polystyrene sphere was used as micro-balloon. Aluminum powder was atomized type whose mean diameter was about 30μm.

Figure 1 presents experimental set-up. The underwater explosion tests were performed in testing tank of 36m in diameter and 8m in depth. Sample explosive was set at the center of testing tank at depth of 4m, and pressure gauge was also set at depth of 4m. Distance between sample explosive and pressure gauge (R) was varied in wide range from 0.05 to 3m, and charge weight (W) was fixed to be 0.1kg. Consequently, scaled distance ($R/W^{1/3}$) was varied from 0.11 to 6.46m/kg$^{1/3}$. Sample explosive was formed in spherical shape whose radius was about 2.7cm, and centrally initiated by No.6 electric detonator. Figure 2 shows the structure of pressure gauge using fluoropolymer as sensing element. Size of fluoropolymer sensing element was 5mm square and 50μm thick. The pressure gauge was filled with insulation oil whose shock impedance was very close to that of water. The pressure gauge was connected to digital oscilloscope through buffer amplifier. Shock wave profile was recorded by digital storage oscilloscope (Nicolet model 460, sampling time 0.2μs), and bubble pulse was recorded by digital storage oscilloscope (Nicolet model Pro90, sampling time 20μs).

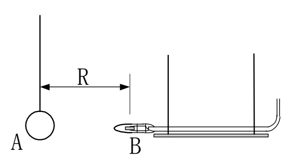


(a) Experimental arrangements

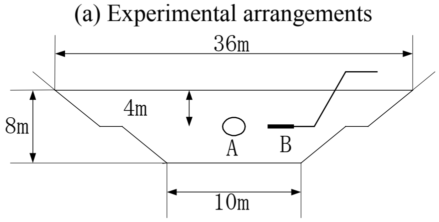


(b) Underwater explosion testing tank

**FIGUER 1. EXPERIMENTAL SET-UP**

(A) Charge, (B) Sensors, (R) Stand off distance

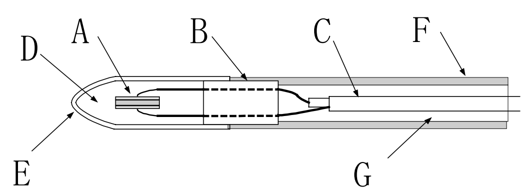


**FIGURE 2. STRUCTURE OF PRESSURE GAUGE**

(A) Sensing element (B) Body
(C) Coaxial cable (D) Insulation oil
(E) Cap (F) Metal tube
(G) Insulation resin

**Table 1 Properties of sample explosives**

| Sample explosive | Density ( $g/cm^3$ ) | Detonation velocity ( m /s ) | Composition | | |
|---|---|---|---|---|---|
| | | | Base emulsion ( wt % ) | GMB ( wt % ) | Al powder ( wt % ) |
| EMX | 1.15 | 3390 | 98.9 | 1.1 | 0 |
| AL-EMX | 1.22 | 3360 | 82.4 | 0.92 | 16.7 |

Shock wave impulse (Is), shock wave energy flux density (EFDs), shock wave energy (Es), and bubble energy (Eb) were determined by following equations, using measured shock wave profile and bubble pulse profile;

$$Is = \int_0^{5\theta} P(t)dt \cdots (1)$$

$$EFDs = \frac{1}{\rho w \cdot Cw} \int_0^{5\theta} P(t)^2 dt \cdots (2)$$

$$Es = \frac{4\pi R^2}{W} EFDs \cdots (3)$$

$$Eb = 6.84 \times 10 \cdot Po^{5/2} \cdot Tb^3 / W \cdots (4)$$

Here, ρw is density of water, Cw is sound velocity of water, θ is characteristic time of shock wave, P(t) is shock wave pressure at time t, Po is total hydrostatic pressure at charge depth and Tb is bubble period.

**RESULTS AND DISCUSSION**

The experimental conditions and results are summarized in Table 2. Underwater shock wave profile was successfully measured even in the condition that peak shock wave pressure exceeded 400MPa. In the case of EMX, measured shock wave energy decreases with the increase of scaled distance in the scaled distance range smaller than $0.3 m/kg^{1/3}$. It is well known that measured bubble energy is an invariant and independent of location of pressure gauge, but this is not true for shock wave energy. During shock wave transmission from the explosive-water boundary to the pressure gauge, one part of shock wave energy is lost by shock heating of surrounding water. When shock wave pressure is higher, loss of shock wave energy is greater. According to the results of previous work [6,7,8], shock wave velocity decays to sound velocity of water, and loss of shock wave energy becomes negligible small at the distance of about 10 charge radii, that is about 0.3m in our experiments. However, in the case of AL-EMX, measured shock wave energy remains constant within the measured scaled distant range. This fact indicates that loss of shock wave energy during shock wave transmission is compensated by shock wave enhancement owing to the late energy release by aluminum reaction in detonation products.

Figure 3 and 4 present typical shock wave profile for EMX and AL-EMX. Pressure decay in shock wave profile of AL-EMX is much slower than that of EMX, and shock wave characteristic time of AL-EMX is much longer than that of EMX owing to the effects of late energy release by aluminum reaction in detonation products. The effects of aluminum reaction on shock wave profile becomes more clear when peak shock wave pressure is higher. When pressure gauge is located very close to the explosive-water boundary, gas bubble of detonation products can arrive at the pressure gauge within observation time. In the case 1 and 11 where pressure gauge is located only about 2.5cm from the explosive-water boundary, gas bubble arrives the pressure gauge in less than 50μs after passage of shock wave, and then pressure gauge can measure pressure of detonation products. Figure 5,6,7 present the relations between peak shock wave pressure (Pmaxs), scaled shock wave impulse ($Is/W^{1/3}$), scaled shock wave energy flux density ($EFDs/W^{1/3}$) and scaled distance. These relations can be expressed by similitude equations[2], and similitude constants and coefficients for EMX and AL-EMX are summarized in Table 3. Peak shock wave pressure of AL-EMX is slightly lower than that of EMX at scaled distance smaller than $1m/W^{1/3}$, and becomes slightly higher than that of EMX at scaled distance larger than $1m/W^{1/3}$ (Figure 5). Scaled shock wave impulse of AL-EMX is about 25% greater than that of EMX (Figure 6), and scaled shock wave energy flux density of AL-EMX is about 15% greater than that of EMX (Figure 7) within measured scaled distance range.

**Table 2 Experimental conditions and results**

| Case | Sample Explosive | Stand off distance (m) | Scaled distance $R/W^{1/3}$ ($m \cdot kg^{1/3}$) | Pmaxs (MPa) | EFDs (m· kPa) | Is (Pa · s) | Es (MJ/kg) | Pmaxb (MPa) | Ib (Pa · s) |
|---|---|---|---|---|---|---|---|---|---|
| 1 | EMX | 0.05 | 0.11 | 464.6 | 2940.0 | 21099 | 0.924 | 46.4 | 80840 |
| 2 | | 0.10 | 0.22 | 213.4 | 723.9 | 9999 | 0.910 | 20.6 | 37713 |
| 3 | | 0.15 | 0.32 | 138.7 | 325.5 | 7975 | 0.920 | 15.7 | 24143 |
| 4 | | 0.20 | 0.43 | 100.1 | 180.2 | 5207 | 0.906 | 9.6 | 17594 |
| 5 | | 0.30 | 0.65 | 57.8 | 72.8 | 3692 | 0.823 | 7.4 | 11263 |
| 6 | | 0.40 | 0.86 | 47.2 | 40.7 | 3082 | 0.818 | 5.7 | 8208 |
| 7 | | 0.50 | 1.08 | 32.0 | 27.4 | 2643 | 0.861 | 4.1 | 6421 |
| 8 | | 1.00 | 2.15 | 17.2 | 7.1 | 1351 | 0.887 | 2.1 | 2996 |
| 9 | | 2.00 | 4.31 | 8.0 | 1.8 | 724 | 0.880 | 1.0 | 1398 |
| 10 | | 3.00 | 6.46 | 5.1 | 0.8 | 503 | 0.866 | 0.7 | 895 |
| 11 | AL-EMX | 0.05 | 0.11 | 383.5 | 3102.5 | 27879 | 0.975 | 58.0 | 90927 |
| 12 | | 0.10 | 0.22 | 178.5 | 824.9 | 13815 | 1.037 | 29.4 | 43430 |
| 13 | | 0.15 | 0.32 | 121.8 | 350.2 | 9665 | 0.990 | 19.1 | 28189 |
| 14 | | 0.20 | 0.43 | 90.3 | 198.0 | 7396 | 0.995 | 13.5 | 20744 |
| 15 | | 0.30 | 0.65 | 59.2 | 88.8 | 5073 | 1.004 | 8.1 | 13464 |
| 16 | | 0.40 | 0.86 | 43.9 | 50.2 | 3882 | 1.009 | 5.9 | 9908 |
| 17 | | 0.50 | 1.08 | 34.8 | 32.3 | 3154 | 1.015 | 4.7 | 7811 |
| 18 | | 1.00 | 2.15 | 16.9 | 8.2 | 1656 | 1.030 | 2.5 | 3731 |
| 19 | | 2.00 | 4.31 | 8.2 | 2.1 | 869 | 1.056 | 1.4 | 1782 |
| 20 | | 3.00 | 6.46 | 5.4 | 0.9 | 596 | 1.018 | 0.9 | 1157 |

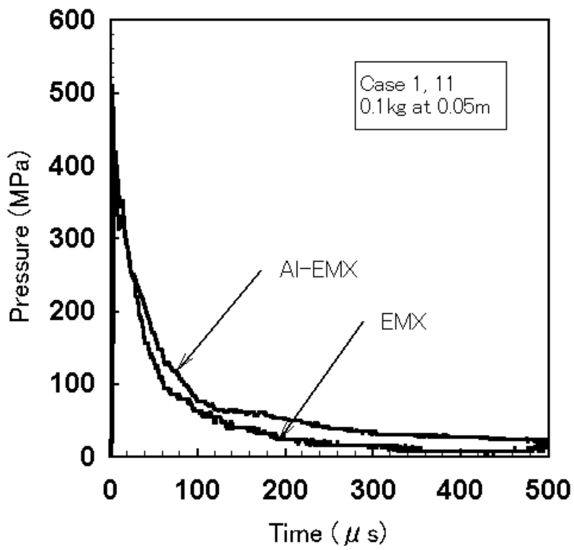


**FIGURE 3. EXAMPLE OF SHOCK WAVE PLOFILE**

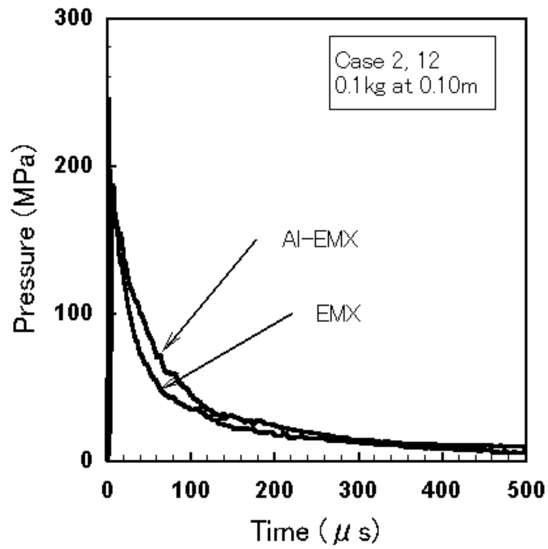


**FIGURE 4. EXAMPLE OF SHOCK WAVE PLOFILE**

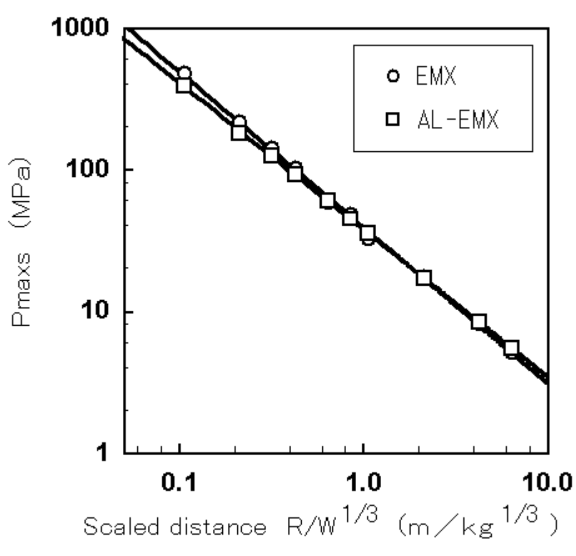


**FIGURE 5. RELATION BETWEEN PEAK SHOCK WAVE PRESSURE AND SCALED DISTANCE**

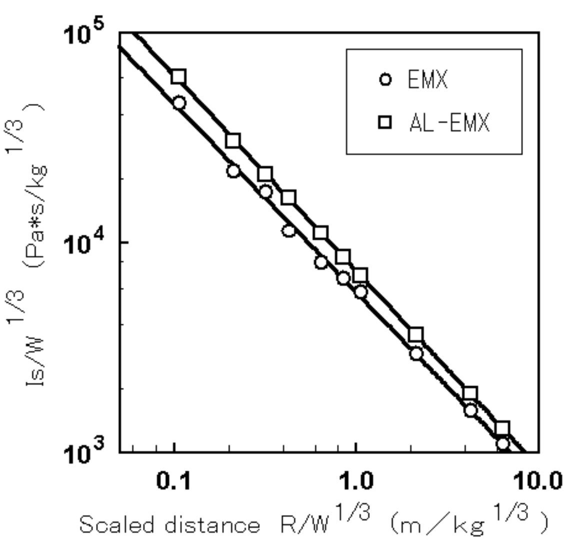


**FIGURE 6. RELATION BETWEEN SCALED SHOCK WAVE IMPULSE AND SCALED DISTANCE**

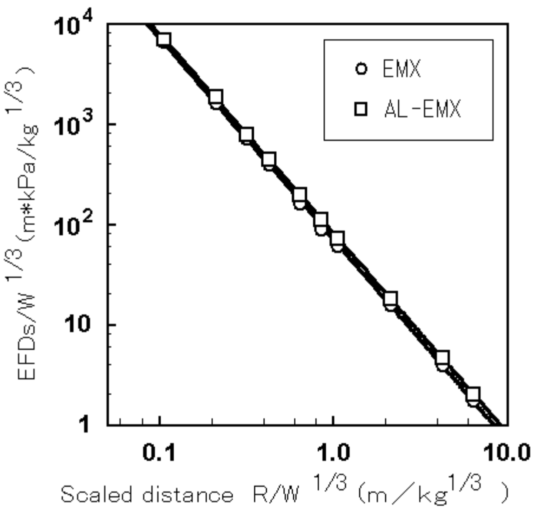


**FIGURE 7. RELATION BETWEEN SCALED SHOCK ENERGY FLUX DENCITY AND SCALED DISTANCE**

Figure 8 shows the examples of bubble pulse profile measured by pressure gauge using tourmaline and fluoropolymer as sensing element. Bubble pulse profile measured by pressure gauge using tourmaline presents important shift in base line to negative pressure after the passage of shock wave, which makes the precise quantitative measurements of bubble pulse pressure and impulse difficult. In contrast, bubble pulse profile measured by pressure gauge using fluoropolymer maintains base line after the passage of shock wave. Figure 9 shows the enlargement of first bubble pulse profile. The duration of first bubble pulse is in the order of 10ms in the measured experimental conditions, and pressure rise is very slow compared with shock wave. Peak pressure of first bubble pulse was determined directly using measured bubble pulse profile.

Bubble pulse impulse (Ib) was calculated using measured bubble pulse profile Pb(t) according to following equation;

$$Ib = \int_{T1}^{T2} P(t)dt \cdots (5)$$

Here, T1 and T2 are respectively the time when bubble pressure increases and decreases to threshold pressure P1. The threshold pressure P1 was selected as 5% of peak bubble pulse pressure considering noise level of measurements. The experimental results are summarized in Table 2. Figure 10 and 11 present the relations between peak bubble pulse pressure (Pmaxb), scaled bubble pulse impulse ($Ib/W^{1/3}$ ) and scaled distance. These relations can be expressed by similitude equations, and similitude constants and coefficients for EMX and AL-EMX are summarized in Table 3. Peak bubble pulse pressure of AL-EMX is about 25% higher than that of EMX, and scaled bubble pulse impulse of AL-EMX is about 20% greater than that of EMX within measured scaled distance range. The experimental results also show that the impulse of first bubble pulse is about 2.5 times greater than shock wave impulse within measured scaled distance range, although peak bubble pulse pressure is only 10~15% of peak shock wave pressure. Consequently, bubble pulse gives important dynamic loading to the underwater structure, and the effects of bubble pulse loading as well as shock wave loading should be considered to study the response of the underwater structure against underwater explosion of explosives. Bubble energy of EMX is 1.8MJ/kg and bubble energy of AL-EMX is 3.0MJ/kg.

**Table 3 Similitude equations of sample explosives**

| Sample explosive | | EMX | | AL-EMX | |
|---|---|---|---|---|---|
| Y | | K | $\alpha$ | K | $\alpha$ |
| Pmaxs | MPa | 39.0 | -1.1 | 37.5 | -1.0 |
| $\theta/W^{1/3}$ | μs/kg $^{1/3}$ | 108 | 0.16 | 154 | 0.10 |
| $Is/W^{1/3}$ | Pa・s/kg $^{1/3}$ | 5760 | 0.90 | 7290 | 0.93 |
| $EFDs/W^{1/3}$ | m・kPa/kg $^{1/3}$ | 70.3 | -2.0 | 80.7 | -2.0 |
| Pmaxb | MPa | 4.57 | -1.02 | 5.68 | -1.02 |
| $Ib/W^{1/3}$ | Pa・s/kg $^{1/3}$ | 15000 | -1.1 | 18210 | -1.07 |

$Y = K\,(R/W^{1/3})^{\alpha}$

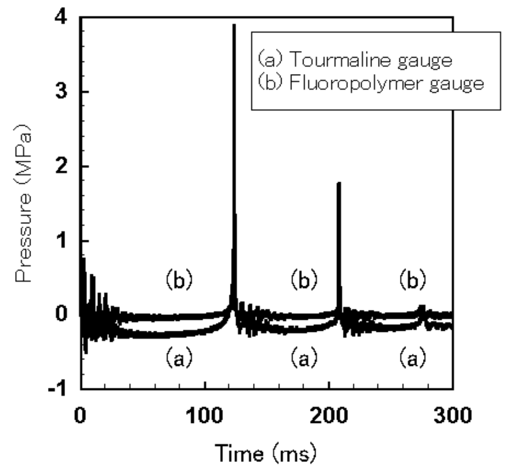


**FIGURE 8. EXAMPLE OF BUBBLE PULSE PROFILE**

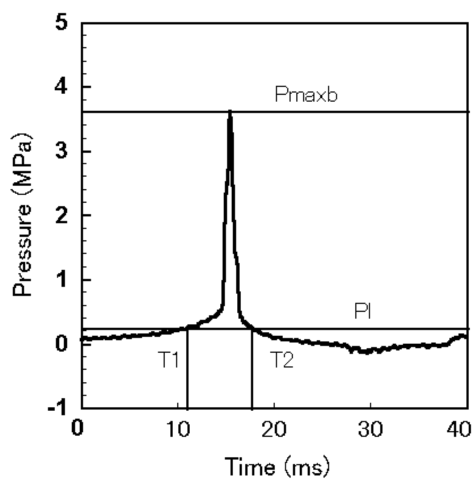


**FIGURE 9. EXAMPLE OF FIRST BUBBLE PULSE PLOFILE**

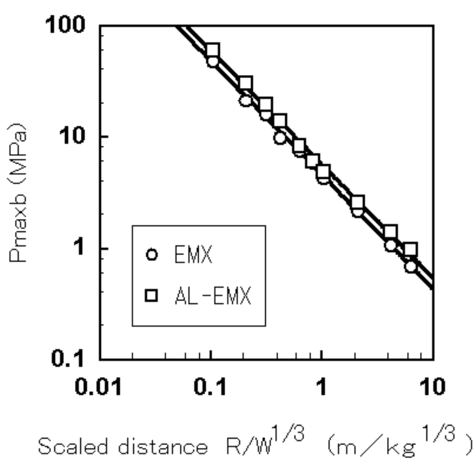


**FIGURE 10. RELATION BETWEEN PEAK BUBBLE PULSE PRESSURE AND SCALED DISTANCE**

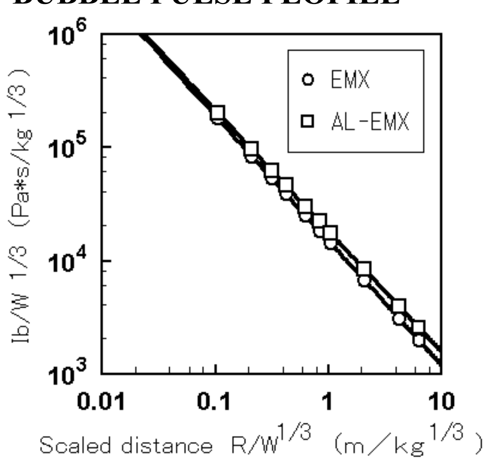


**FIGURE 11. RELATION BETWEEN SCALED BUBBLE PULSE IMPULSE AND SCALED DISTANCE**

## CONCLUSIONS

To measure underwater shock wave profile at the location very close to the explosive-water boundary, pressure gauge using fluoropolymer as sensing element was developed. Underwater shock wave profile was successfully measured in high pressure range where peak shock wave pressure exceeded 400MPa for EMX and AL-EMX. Bubble pulse profile was also precisely measured using pressure gauge using fluoropolymer. Following experimental results were obtained;

(1) In the case of EMX, shock wave energy decreases with the increase of scaled distance in the scaled distance range smaller than 0.3 $m/kg^{1/3}$, due to the loss of shock wave energy by shock heating of surrounding water. However, in the case of AL-EMX, shock wave energy remains constant owing to shock wave enhancement due to the late energy release by aluminum reaction in detonation products.

(2) Peak shock wave pressure of AL-EMX is almost same as that of EMX. Scaled shock wave impulse of AL-EMX is about 25% greater than that of EMX, and scaled shock wave energy flux density is about 15% greater than that of EMX within measured scaled distance range.

(3) Peak bubble pulse pressure of AL-EMX is about 25% higher than that of EMX, and scaled bubble impulse is about 20% greater than that of EMX within measured scaled distance range.

(4) The impulse of first bubble pulse is about 2.5 times greater than that of shock wave impulse, although peak pressure of first bubble pulse is only 10~15% of peak shock wave pressure.

(5) The relations between peak shock wave pressure, scaled shock wave impulse, scaled shock wave energy flux density, peak bubble pulse pressure, scaled bubble pulse impulse and scaled distance are formulated in similitude equations.

## REFERENCES

1. Cole, R. H., “Underwater explosions”, Dover Publications, New York (1948).
2. Roth, J. , “Underwater explosions” in Encyclopedia of Explosives and Related Items, Vol. 10, pp. U38-81, U. S. Army Research and Development Command, Dover, New Jersey (1983).
3. Murata, K., Takahashi, K., Kato, Y. and Murai, K., “Development of pressure gauge using PVDF copolymer for underwater shock measurement”, in APS Proceedings of Shock Compression of Condensed Matter-1995, American Institute of Physics, pp. 1093-1096 (1996).
4. Murata, K., Takahashi, K. and Kato, Y., “Measurement of underwater shock wave by fluoropolymer sensor”, Proceedings of 23rd International Pyrotechnics Seminar, pp. 548-560 (1997).
5. Murata, K., Takahashi, K. and Kato, Y., “Precise measurements of underwater explosion phenomena by pressure sensor using fluoropolymer”, Journal of Materials Processing Technology, 85, pp. 39-42 (1999).
6. Sternberg, H. M. and Walker, W. A., “Calculated flow and energy distribution following underwater detonation of a pentolite sphere”, The Physics of Fluids, 14, pp. 1869-1878 (1971).
7. Hantel, L. W. and Davis, W. C., “Spherical explosion in water”, Proceedings of 5th Symposium (International) on Detonation, ACR-184 Office of Naval Research, Arlington, Virginia, pp. 599-604 (1970).
8. Sanchidrian, J. A., “Numerical modeling evaluation of underwater energies”, Propellants, Explosives, Pyrotechnics, 23, pp. 301-308 (1998).